ACS Sustainable Chemistry & Engineering

pubs.acs.org/journal/ascecg

Research Article

Eight-Fold Intensification of Electrochemical Azidooxygenation with a Flow-Through Electrode

Shichen Guo, Myung Jun Kim, Juno C. Siu, Natalia von Windheim, Ken Gall, Song Lin, and Benjamin J. Wiley*

Cite This: https://doi.org/10.1021/acssuschemeng.2c01525

Read Online

ACCESS | Metrics & More | Article Recommendations | Supporting Information

ABSTRACT: Finding ways to reduce reactor volume while increasing product output for electro-organic reactions would facilitate the broader adoption of such reactions for the production of chemicals in a commercial setting. This work investigates how the use of flow with different electrode structures impacts the productivity (i.e., the rate of product generation) of a TEMPO-mediated azidooxygenation reaction. Comparison of a flow and batch process with carbon paper (CP) demonstrated a 3.8-fold-higher productivity for the flow reactor. Three custom carbon electrodes, sintered carbon paper (S-CP), carbon nanofiber (CNF), and composite carbon microfiber-nanofiber (MNC), were studied in the flow reactor to evaluate how changing the electrode structure affected productivity. Under the optimum conditions, these electrodes achieved productivities 5.4, 6.5, and 7.8 times higher than the average batch reactor, respectively. Recycling the outlet from the flow reactor with the MNC electrode back into the inlet achieved an 81% yield in 36 min, while the batch reactor obtained a 75% yield in 5 h. These findings demonstrate that the productivity of electro-organic reactions can be substantially improved through the use of novel flow-through electrodes.

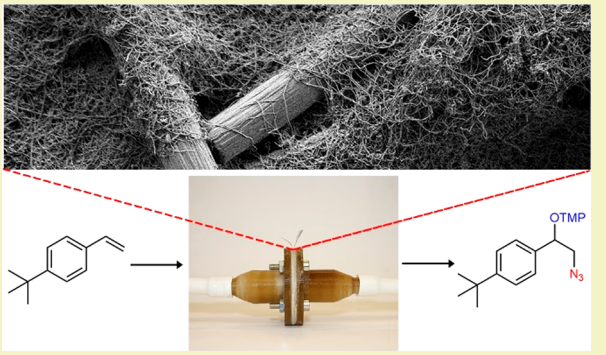

KEYWORDS: *electro-organic, flow reactor, electrode, carbon microfiber, carbon nanofiber*

INTRODUCTION

Organic electrochemistry involves the application of a voltage across and current through a solution to achieve the desired oxidation or reduction of organic molecules. By changing the applied voltage, one can achieve a broad range of reactivity for activating inert chemical bonds or suppressing unwanted reactions. Stoichiometric quantities of potentially hazardous oxidants and reductants can be eliminated by using electrons and holes to provide redox equivalents.[1−7] The advantages of organic electrochemistry have motivated a renewed interest in its application to solving difficult synthetic problems.[8,9]

Despite its advantages, organic electrochemistry is not widely used for the production of pharmaceuticals. One hurdle to adoption by medicinal chemists is accessibility and standardization. These issues are being addressed through the development of instruments such as the ElectraSyn 2.0 system and platforms for high-throughput experimentation.[10−14]

A second hurdle exists for process chemists: scaling up promising electrochemical reactions to produce kilograms in a small amount of time and space.[15] In this case, a key figure of merit is the productivity, i.e., amount of product produced per unit time. The productivity can be normalized to the electrode area to compare different electrode configurations. One approach to the problem of scale-up is to create electrochemical flow cells in which the reaction solution flows between parallel plates.[9,16−20] For example, the long-channel (2 m), spiral "Ammonite" flow cell has reported a production rate of 0.2 g h^{-1} per cm^2 of electrode area for the methoxylation of *N*-formylpyrrolidine.[17] However, such parallel plate reactors do not take advantage of the much-higher volumetric surface areas of 3D porous electrodes,[21] such as metal mesh,[22] metal foam,[23] graphite felt,[24,25] carbon paper (CP),[26] and reticulated vitreous carbon (RVC).[27−29] For reactions that are limited by charge transfer, the higher volumetric surface area of a 3D porous electrode can theoretically increase the rate of the reaction in proportion to its higher electrode surface area.[30] For reactions that are limited by transport of the reactant to the electrode surface, incorporating flow across or, better yet, through a porous electrode can increase the rate of the reaction to an even greater extent.[21,31] In both cases, the use of flow-through 3D porous electrodes can enable intensification of the electro-

Received: March 14, 2022
Revised: May 9, 2022

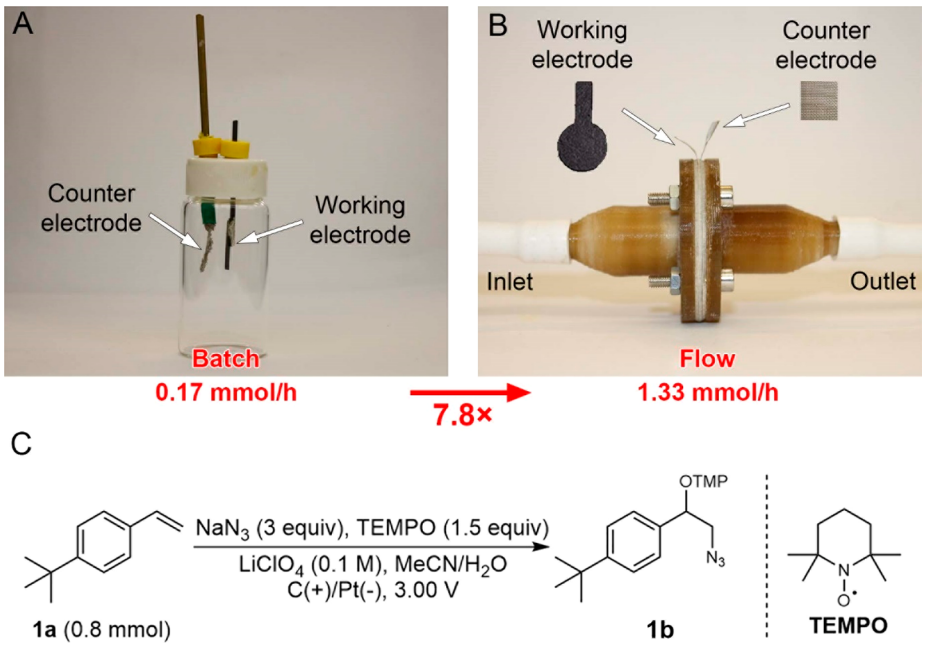

Figure 1. (A) Image of a batch reactor. (B) Image of a 3D-printed PEKK flow cell. The values below panels (A) and (B) are the maximum productivity (mmol of product per hour) for azidooxygenation in each reactor. (C) Scheme of TEMPO-mediated azidooxygenation reaction using 4-*tert*-butylstyrene (**1a**) for the production of 1-(2-azido-1-(4-(*tert*-butyl)phenyl)ethoxy)-2,2,6,6-tetramethylpiperidine (**1b**).

chemical reaction, thereby minimizing the time and space required to produce sufficient quantities of the desired product.[31−35]

Since organic electrochemists nearly always utilize commercially available electrodes, there are many reactions for which it is unclear to what extent changing the structure of an electrode can improve the productivity of an electro-organic reaction.[31] We have recently explored how the use of a copper nanowire felt in a flow-through reactor can improve the productivity of an electrochemical process.[31] The higher surface area and mass-transport coefficient enabled a 4.2-fold increase in the productivity of a cyclization reaction. However, most electro-organic reactions consist of oxidations that would dissolve the copper nanowire electrode. In addition, many electro-organic reactions use a mediator, such as 2,2,6,6-tetramethylpiperidine N-oxyl (TEMPO), to facilitate the desired transformation.[36−38] It is not clear to what extent changing the structure of the electrode can increase the rate of electro-organic reactions that utilize a mediator.

In this work, we explore how the use of flow and changing the structure of a carbon-based electrode can improve the productivity of TEMPO-mediated azidooxygenation of alkenes (see Figure 1).[37] We focused our study on the TEMPO-mediated azidooxygenation of alkenes for three reasons: (1) TEMPO is a widely used mediator, so the extent to which the productivity of this reaction can be improved may apply to other TEMPO-mediated electro-organic reactions or to reactions involving other mediators, (2) the aminoalcohol-type molecules that can be obtained via this reaction are prevalent among pharmaceuticals,[39] and (3) this reaction proceeds under very mild conditions and offers broader substrate scope than alternatives.[40−42] We focus on the use of carbon as an electrode material, because it is relatively inexpensive, offers high corrosion resistance, can be fabricated into structures at a variety of length scales, and is commonly used in electro-organic reactions as an anode or cathode.[37,43−49]

CP was used as the benchmark anode because it has the largest specific surface area among commercially available flow-through electrodes[31] and has previously been used in electro-organic reactions.[50−54] We find that switching from a batch to flow reactor with commercially available CP as an electrode can improve the productivity of the reaction by 3.8 times. Changing from a standard CP electrode to a composite microfiber-nanofiber electrode (MNC) improved the productivity of the flow-cell reaction 2.1 times, for a total increase of 7.8 times relative to the batch system with CP electrode. While the batch reactor achieved a maximum yield of 75% in 5 h, the flow reactor with the composite electrode achieved a maximum yield of 81% in 36 min, and a production rate of 0.72 g h^{-1} per cm^2 of electrode area. This production rate per cm^2 of electrode area represents a 3-fold increase over the highest previously reported values for an electro-organic reaction.[17] This work demonstrates that the use of a flow-through electrode can improve the productivity of a TEMPO-mediated reaction relative to a batch synthesis, and that the use of MNC electrode with a higher surface area can further improve the productivity of the reaction relative to a CP electrode. This work further demonstrates that the productivity of flow-reactors incorporating 3D porous electrodes can greatly exceed that of nonporous parallel-plate flow reactors for the production of organic chemicals.

RESULTS AND DISCUSSION

Batch Versus Flow with Carbon Paper. A customized batch reactor (Figure 1A) and flow cell (Figure 1B) were fabricated to evaluate the effect of the flow-through process on the productivity of a TEMPO-mediated azidooxygenation reaction (Figure 1C). The batch reactor consisted of a 20 mL glass vial with three holes drilled into the cap. The anode was a 0.5 cm × 2.0 cm × 0.036 cm piece of CP connected to a

https://doi.org/10.1021/acssuschemeng.2c01525
ACS Sustainable Chem. Eng. XXXX, XXX, XXX−XXX

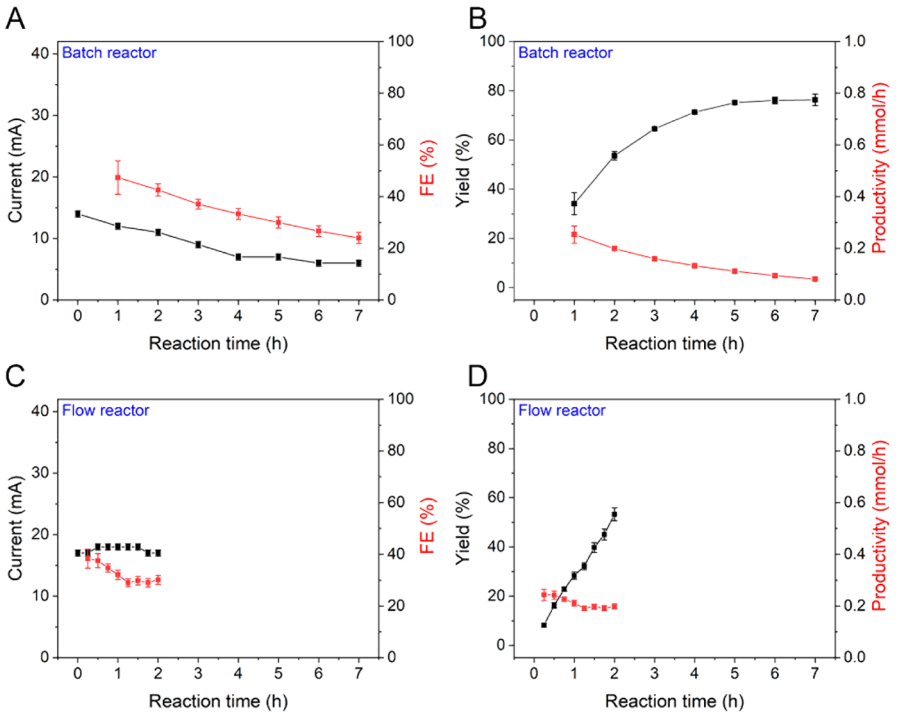

Figure 2. (A) Current and faradic efficiency (FE), and (B) yield and productivity of azidooxygenation with carbon paper (CP) in the batch reactor. (C) Current and FE, and (D) yield and productivity of azidooxygenation with CP in the flow reactor with a low flow rate of 0.1 mL/min.

graphite rod. The cathode was a platinum mesh connected to a brass rod. The exposed surface areas of anode and cathode in solution were 0.5 cm^2, and the spacing of the two electrodes was ~5 mm. The polyetherketoneketone (PEKK) flow cell was fabricated by 3D printing two separate pieces that can be connected to rubber tubing via a zip tie. The two halves of the flow cell were then assembled with gaskets and electrodes between them and screwed together (see Figure S1 in the Supporting Information for an image of the disassembled reactor components), forming the following structure: inlet/gasket/working electrode/gasket/counter electrode/gasket/outlet. The anode was a piece of CP prepared by cutting (see Figure S2 in the Supporting Information for shape of the electrode) and the cathode was Pt mesh. The exposed surface areas of anode and cathode are both 0.5 cm^2, an area controlled by the hole on the gasket. CP was used as the anode because carbon is corrosion resistant and CP has the largest specific surface area among commercial flow-through electrodes.[31] Pt mesh was used as the cathode due to the low overpotential required to reduce water to hydrogen on Pt. The spacing between the anode and cathode was 0.8 mm, which was the thickness of the gasket.

The azidooxygenation reaction was adopted and modified from previous work.[37] For both the batch and flow reaction, 4-*tert*-butylstyrene (0.8 mmol, 1.0 equiv) and TEMPO (1.2 mmol, 1.5 equiv) were added to MeCN (14.0 mL) solution with 0.1 M $LiClO_4$. An aqueous solution of NaN_3 (2.4 mmol, 3.0 equiv) was then added to the mixture. Additional experimental details are given in the Supporting Information. During the TEMPO-mediated azidooxygenation, the TEMPO radical is oxidized to $TEMPO^+$ and water is reduced to hydrogen. The $TEMPO^+$ then forms the charge-transfer complex TEMPO-N_3 and facilitates the formation of an azidyl radical. Both azidyl and TEMPO radicals were then successively added onto the alkene to form the final product (Figure S3 in the Supporting Information).[37,55]

For an electro-organic reaction, the applied potential should be high enough to ensure a high rate of charge transfer while being low enough to avoid unwanted reactions. To determine the ideal potential window, we first performed azidooxygenation with cell potentials between 2.2 V and 3.4 V, and with two different flow rates (0.5 and 2.0 mL/min). As shown in Figure S4A in the Supporting Information, under both flow rates, the productivity increased by more than two times as the potential was increased from 2.2 V to 3.0 V. At 3.4 V, the productivity did not increase significantly, indicating the reaction had become mass-transport-limited between 3.0 V and 3.4 V. In addition, the background current doubled when the voltage was increased from 3.0 V to 3.4 V (see Figure S4B in the Supporting Information). An increase in background current decreases the faradaic efficiency and potentially increases unwanted reaction byproducts. Therefore, 3.0 V was chosen as the optimum applied potential for the azidooxygenation reaction in our reactors.

Figure 2A shows the current and faradic efficiency (FE) for the batch reactor. Both the current and FE decrease with time for the batch reactor, because, as the reactants are consumed, the rate at which the reactant is transported to the electrode decreases. Figure 2B shows that the yield for the batch reactor increases until it reaches a plateau at ~5 h, at which point the yield is 75%. The productivity for the batch reaction starts at 0.23 mmol/h but decreases to 0.11 mmol/h at 5 h, because of the decrease in the concentration of reactants with time.

Figure 2C illustrates how the flow reactor is fundamentally different from the batch reactor. The flow reactor is fed with a constant concentration of reactant, so it is able to maintain a relatively high and constant current with time. This constant feed of reactant allows the flow reactor to maintain a more consistent productivity, which starts at 0.24 mmol/h, before

https://doi.org/10.1021/acssuschemeng.2c01525
ACS Sustainable Chem. Eng. XXXX, XXX, XXX−XXX

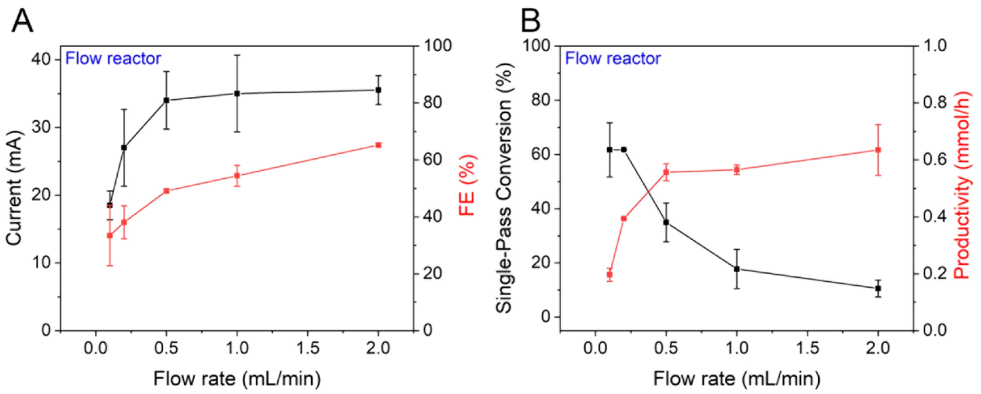

Figure 3. (A) Current and faradic efficiency (FE), and (B) yield and productivity of azidooxygenation with CP in the flow reactor, as a function of flow rate.

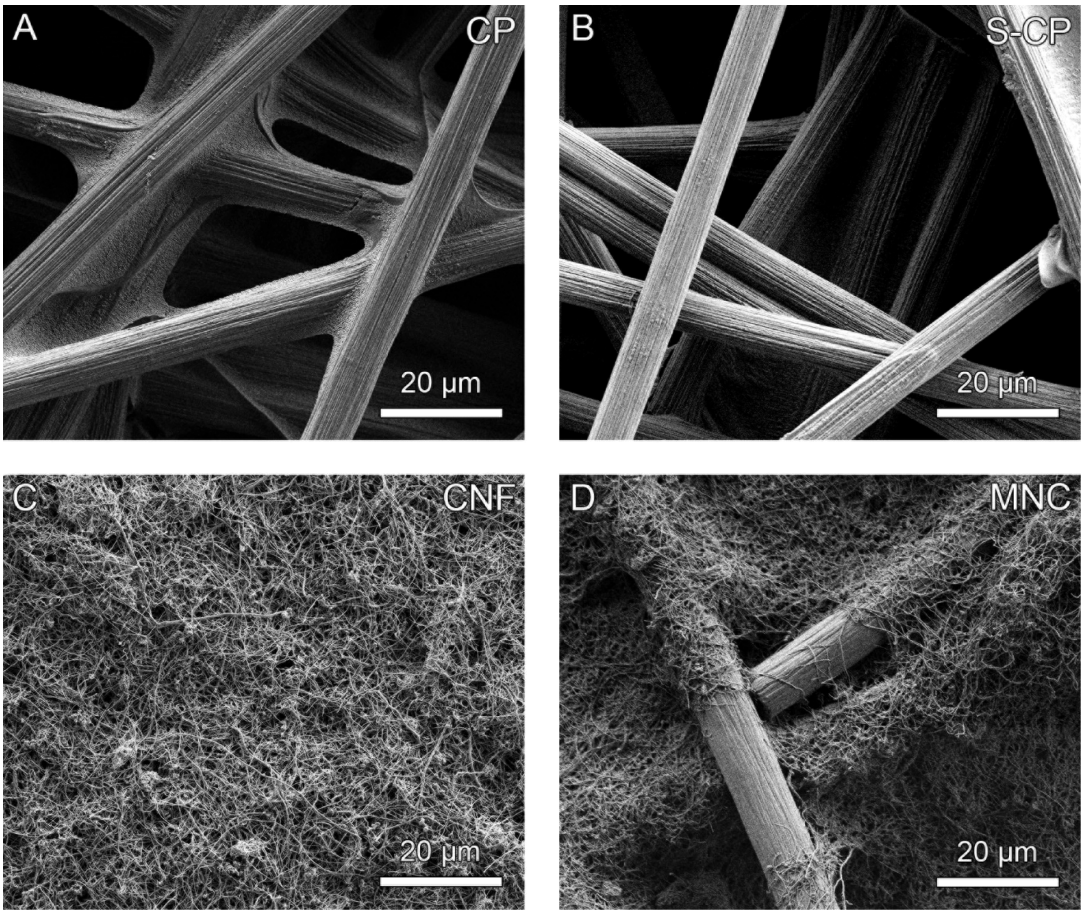

Figure 4. SEM images of different carbon electrodes: (A) CP, (B) sintered carbon paper (S-CP), (C) carbon nanofiber (CNF), (D) carbon microfiber-nanofiber composite (MNC).

decreasing to 0.19 mmol/h. We ascribe this decrease to a buildup of NaOH on the surface of the anode, which we will speak of more later. At this low flow rate of 0.1 mL/min, the productivity during the first 2 h is similar to that of the batch reactor, suggesting that the larger distance between the electrodes in the batch reactor is not limiting its productivity. Since the productivity in the two reactors is similar at this low flow rate, the yield at 2 h for the flow reactor (53%) is similar to the yield obtained in the batch reactor at the same time point (52%).

Since the reaction is limited by transport of reactants to the electrodes, higher currents and faradaic efficiencies can be obtained by increasing the flow rate (Figure 3A).[24,56−58] The higher current and higher FE translates to a higher productivity (Figure 3B). At the highest flow rate we tested (2.0 mL/min), a productivity of 0.64 mmol/h could be obtained. This is an increase of 278% relative to the best productivity for the batch reactor and 581% relative to the productivity for the batch reactor when the reaction complete. However, a higher flow rate also decreases the residence time and therefore decreases the yield for a single pass of reactant through the electrode. We

https://doi.org/10.1021/acssuschemeng.2c01525
ACS Sustainable Chem. Eng. XXXX, XXX, XXX−XXX

will later show that multiple passes through the flow reactor produces yields comparable to the batch reactor in a small fraction of the time.

Fabrication and Characterization of Carbon Electrodes with Higher Surface Areas. After clearly establishing the extent to which the flow reactor can improve the productivity of TEMPO-mediated azidooxygenation with a CP anode, we next sought to determine how changing the structure of the electrode can further improve its productivity. Three additional carbon electrodes were prepared: sintered carbon paper (S-CP), carbon nanofiber (CNF), and MNC. The CNF electrode and MNC electrode were prepared by dispersing 10 mg of fibers in a liquid suspension, filtering the suspensions through CP, dipping CP with the filtrate into a glucose solution, drying in an oven overnight, and annealing at 1000 °C for 1 h under argon to improve the conductivity and mechanical stability of the electrode. Since the temperatures required for graphitization of carbon (>2000 °C)[59,60] are difficult to obtain with conventional laboratory furnaces, we relied on the addition of glucose to enable low-temperature graphitization.[61] The optimum glucose concentration was that which maximized the conductivity without making the electrode so brittle that it easily fractured (Figure S5 in the Supporting Information). Since both electrodes used CP as the substrate and could not be removed from the substrate, S-CP electrodes were also prepared under the same conditions for comparison to evaluate what benefits in productivity could be obtained by adding the nanofibers or microfiber/nanofiber composite. The scanning electron microscopy (SEM) images of the CP, S-CP, CNF, and MNC electrodes are shown in Figure 4. Note that the CP contained 5 wt % polytetrafluoroethylene (PTFE).[62] The primary difference between CP and S-CP was the morphology of the PTFE particles at the edge of the carbon fiber (Figure S6 in the Supporting Information). After sintering, the PTFE particles merged into a solid mass. SEM images of cross sections of the electrodes show the thicknesses of the CP/S-CP, CNF, and MNC electrodes are 0.360, 0.685, and 0.717 mm, respectively (Figure 5). A detailed description of electrode fabrication is provided in the Supporting Information.

The physical properties of the four electrodes are summarized in Figure 6 and Table S1 in the Supporting Information. All electrodes had a similarly high conductivity. The electrochemically active surface area (ECSA) was measured with the PEKK flow cell assembled with a Ag/$AgNO_3$ reference electrode (Figure S7 in the Supporting Information) and calculated with the double-layer capacitance method (Figure S8 in the Supporting Information).[63] The ECSA of S-CP is 1.1×10^3 cm^2/cm^3, which is 16 times higher than that of CP. This increase in surface area may be related to the pyrolysis of PTFE[64] and the assistance of glucose.[61] The ECSA of MNC and CNF is 7.8×10^3 cm^2/cm^3 and 1.8×10^4 cm^2/cm^3, respectively, which is 113 times and 261 times higher than that of CP. The higher surface area of MNC and CNF electrodes is due to the smaller diameters of the constituent nanofibers (0.1 μm), relative to carbon microfibers (10 μm).

The permeability of a flow-through electrode is an important characteristic because it determines the flow rate that can be achieved for a given pressure drop, as described by Darcy's law:[65,66]

$$u = -\frac{k}{\mu}\frac{\Delta p}{L} \quad (1)$$

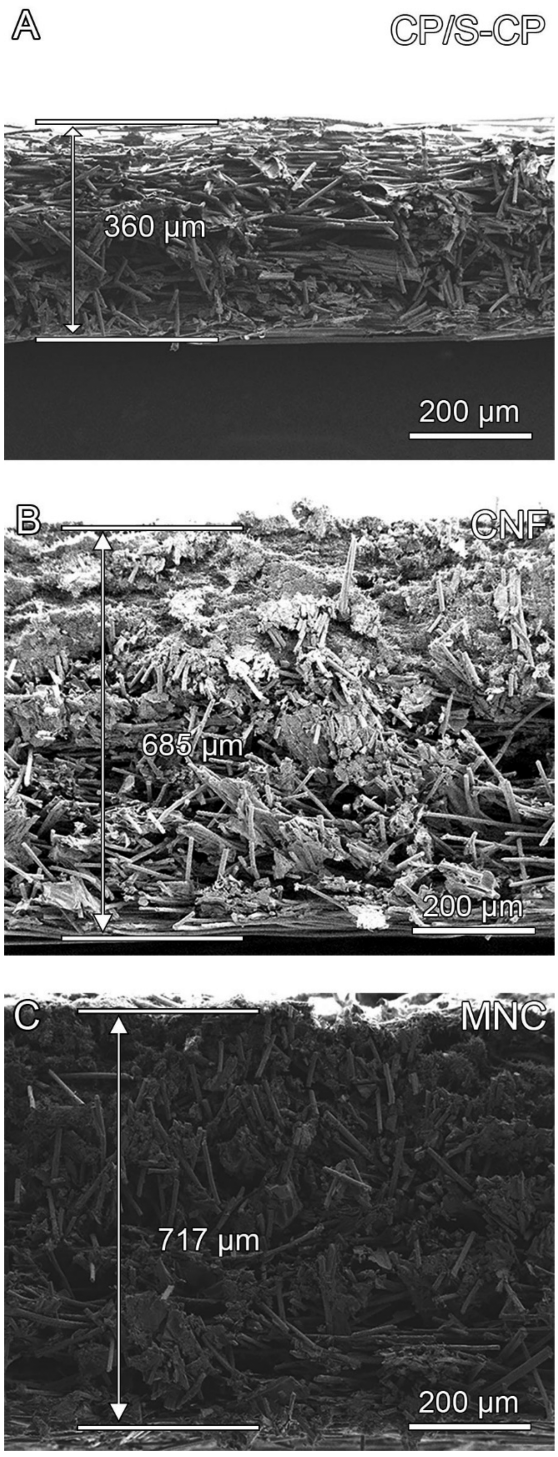

Figure 5. Thickness of different carbon electrodes measured by the cross-section SEM images: (A) CP and S-CP, (B) CNF, and (C) MNC.

where u is the superficial velocity, k is the permeability, μ the viscosity, Δp is the pressure drop across the electrode, and L is the thickness of the electrode. If the permeability of an electrode is too low, then it may not be possible to achieve a desired flow rate through the electrode because the necessary pressure will cause the reactor to leak or will cause the electrode to break.

The permeability of the electrodes was determined by linear fits to measurements of the pressure drop across the electrode

https://doi.org/10.1021/acssuschemeng.2c01525
ACS Sustainable Chem. Eng. XXXX, XXX, XXX−XXX

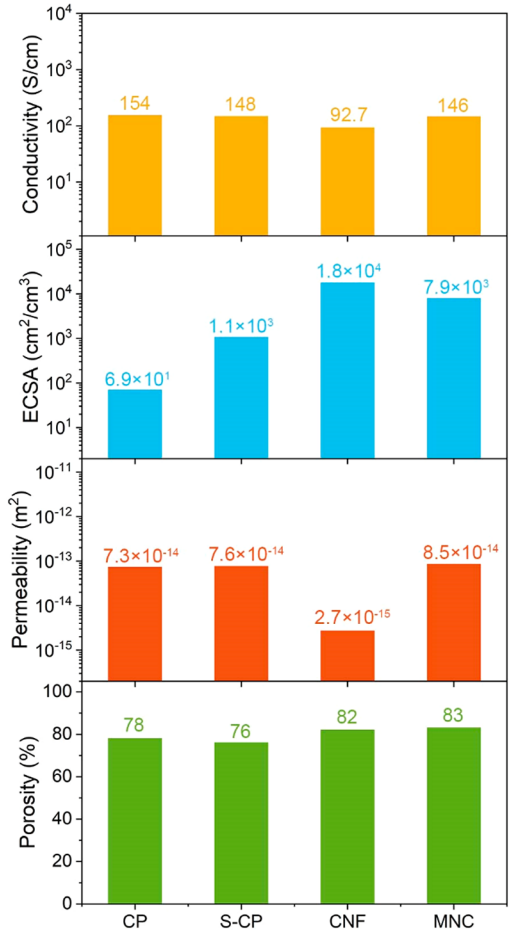

Figure 6. Conductivity, electrochemical active surface area (ECSA), permeability, and porosity of different carbon electrodes.

for a given flow rate (see Figure S9 in the Supporting Information).[65−67] The CP, S-CP, and MNC electrodes have a similar permeability. The permeability of the CNF electrode is 31 times lower than that of MNC. This lower permeability (k) can be understood from the Kozeny−Carman (KC) equation:

$$k = \frac{d^2\varepsilon^3}{16K_C(1-\varepsilon)^2} \tag{2}$$

where d is the diameter of the fibers, ε the porosity of the electrode, and K_c is the Kozeny constant, which is a function of the pore geometry and tortuosity.[66] The KC equation indicates that the permeability will decrease as the fiber diameter and electrode porosity each decrease. As the porosity of the CNF electrode is similar to the other electrodes, the cause for the lower permeability can be ascribed to the much smaller diameter of the nanofibers.

Flow Reactor Performance with Higher Surface Area Electrodes. The current, FE, yield and productivity of azidooxygenation with S-CP, CNF, and MNC is shown in Figure 7. SEM images of the electrodes before and after the reaction under the flow rate that achieved the maximum productivity indicate the electrodes are stable under the reaction conditions (Figure 4, as well as Figure S10 in the Supporting Information). Sintering the CP led to an improvement in performance relative to CP without sintering because of a higher ECSA. The higher surface area of the CNF electrode also enabled it to achieve a higher current, FE, yield, and productivity than CP under the same conditions. Similar currents were obtained with the MNC electrode as the CNF, but the MNC had a higher FE, and thus higher yield and productivity. It is unclear why the CNF exhibited a lower FE. It may be related to the lower permeability of the electrode, which may cause the reactant to transport across the electrode surface to be uneven. This, in turn, may lead to depletion of the reactant in pockets of the electrode and greater production of undesirable side products. Thus, the MNC electrode seems

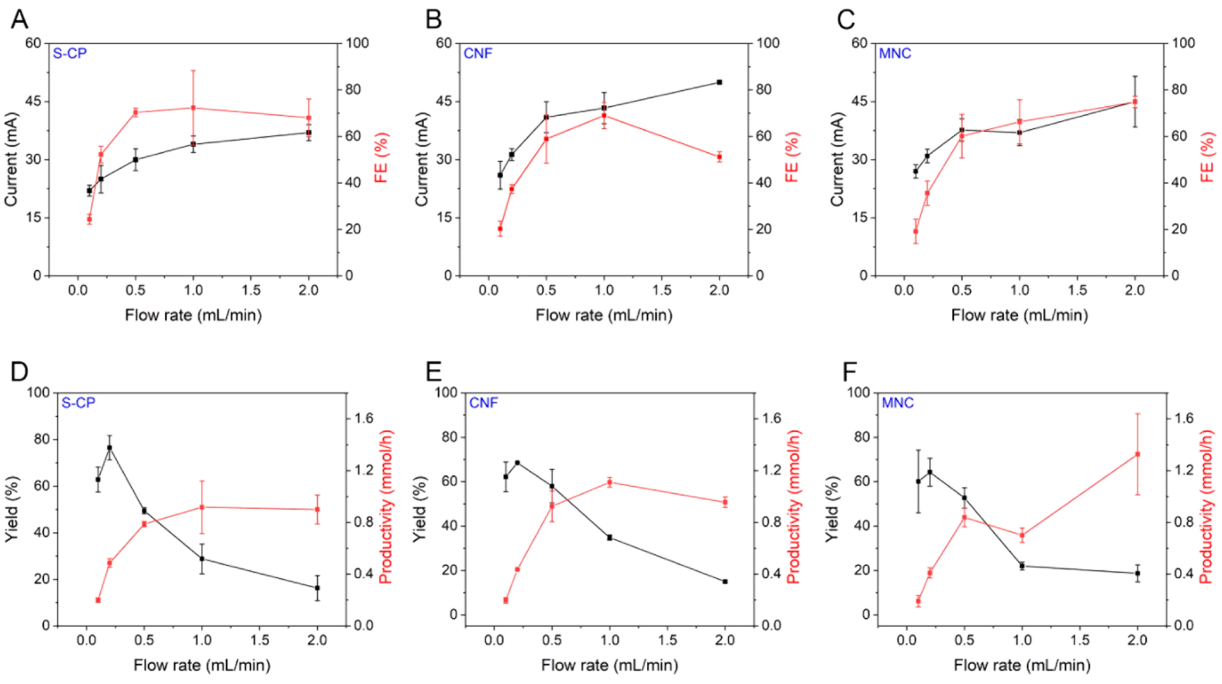

Figure 7. Current, FE, yield, and productivity of azidooxygenation for flow reactors using (A, D) S-CP, (B, E) CNF, and (C, F) MNC.

https://doi.org/10.1021/acssuschemeng.2c01525
ACS Sustainable Chem. Eng. XXXX, XXX, XXX−XXX

to strike a balance between higher surface area while maintaining a sufficient permeability to achieve a high mass transport of reactant.

The average productivity for the batch reaction with CP is compared to the optimum productivities for the flow reactors with the four different electrodes in Figure 8A. We compared

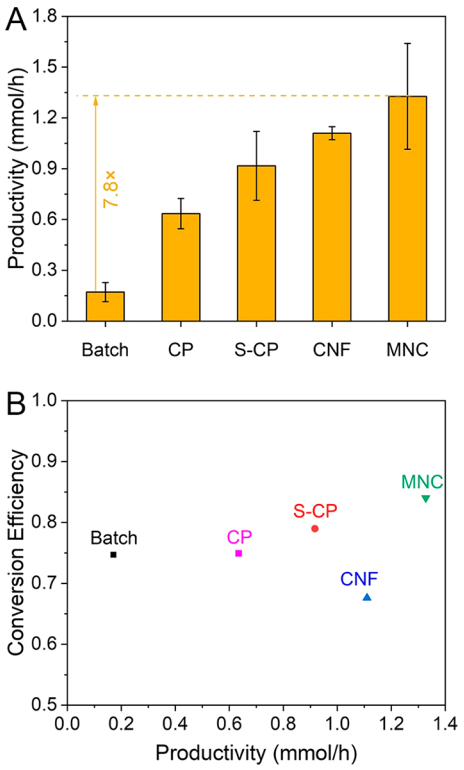

Figure 8. (A) Productivity of the azidooxygenation reaction in a batch reactor with CP and in a flow cell with four different carbon electrodes. (B) Plots of conversion efficiency versus productivity of CP in a batch reactor and with different carbon electrodes in a flow cell.

the average productivity for the batch reactor since its productivity is less constant than the flow reactors. The higher surface areas of the S-CP, CNF, and MNC electrodes enable them to achieve productivities 5.4, 6.5, and 7.8 times higher than the average batch productivity, respectively. Relative to commercially available CP, the S-CP, CNF, and MNC electrodes improve the reactor productivity by factors of 1.4, 1.7, and 2.1, respectively.

Figures 3B and 7D–F show that the productivity increases as the flow rate increases, but the yield decreases. The decreasing yield in this case is primarily due to a shorter residence time of the reactant within the porous electrode. The shorter residence time can lead to a higher amount of reactant that does not participate into the reaction. Therefore, in order to estimate the efficiency with which each electrode converts reactant to product, we calculate and plot the values of product/(alkene consumed) for the batch reactor and four carbon electrodes. Since this value is calculated as product out/(reactant in − reactant out) and is analogous to an energy efficiency, we refer to it as the conversion efficiency. Values of conversion efficiency are plotted against productivity in Figure 8B, and their number values are listed in Table S2 in the Supporting Information. Figure 8B shows that the MNC electrode exhibits both high productivity and high conversion efficiency, whereas the CNF electrode exhibits high productivity but lower conversion efficiency. Based on the results from Figure 8, we can conclude that the MNC electrode has the best performance for the azidooxygenation reaction among the electrodes tested.

Increasing Yield with Recycling. We note that while the productivity increases with flow rate, the single-pass yield decreases. The reaction yield can be increased by simply recycling the output of the reactor back into the syringe used at the inlet. This experiment was performed for the MNC electrode for six cycles. The same reaction solution and electrode were used for each cycle. Each cycle required 6 min to pump the reactant through the electrode, resulting in a total reaction time of 36 min. During this process, we noticed that the yield increased slowly after each cycle and only achieved a 37% yield after six cycles (Figure S11A in the Supporting Information). A small leak was also observed after the third cycle. After disassembling the flow cell, we observed the anode was covered by a white salt (Figure S11B in the Supporting Information). We determined this salt to be primarily NaOH, based on the pH value of the salt dissolved in water and the balanced reaction equation (Figure S3 in the Supporting Information). Thus, it appears NaOH was precipitated from the reaction solution because of the low solubility in acetonitrile, and the deposition of the NaOH on the electrode surface decreased the performance of the electrode.

In order to remove NaOH from the electrode and improve the recycling performance, deionized water was passed through the electrode at a flow rate of 2 mL/min for 2 min after each cycle. This electrode wash was able to remove the visible deposit of NaOH from the electrode (see Figure S11C in the Supporting Information). The curves of yield versus reaction time for the flow reaction are compared to the batch reaction in Figure 9A. Figure S12A in the Supporting Information plots the same information, except the time for washing the flow reactor electrode is included. After six cycles of recycling with a reaction time of 36 min (46 min with washing steps), the azidooxygenation reaction in the flow cell was complete and achieved a yield of 81%. In comparison, the batch reaction took 5 h (eight times longer) to achieve a yield of 75%. The overall productivity in the flow cell after 6 cycles was 1.00 mmol/h, compared to a productivity of 0.11 mmol/h in the batch reactor after 5 h when the reaction was complete. The microfiber–nanofiber layer remained on the CP layer after the reaction (Figure S11C in the Supporting Information). The weight of the MNC electrode before and after each recycling reaction varied by no more than 0.4 mg (0.8%; see Figure S13 in the Supporting Information), indicating that the electrode remained intact over the course of the reactions.

Extension to a More Difficult Substrate. Finally, we extend the same reaction system, without further optimization, to a substrate that is more difficult to convert, 4-phenyl-1-butene (**2a** in Figure 9).[37] Generally, electrochemical flow reactors improve reactions that are kinetically fast and mass-transport-limited to a greater extent than reactions that are relatively slow and reaction-rate-limited,[31] because of their ability to increase the rate of mass transport to the electrode. Therefore, we expect the reduction in reaction time to be less dramatic for **2a** than for **1a**. For **2a**, the batch reactor with the CP anode achieved a yield of 34% in 5 h with a productivity of 0.05 mmol/h. The flow reactor with the MNC anode achieved a higher yield of 40% after 21 cycles with a reaction time of 2 h

https://doi.org/10.1021/acssuschemeng.2c01525
ACS Sustainable Chem. Eng. XXXX, XXX, XXX–XXX

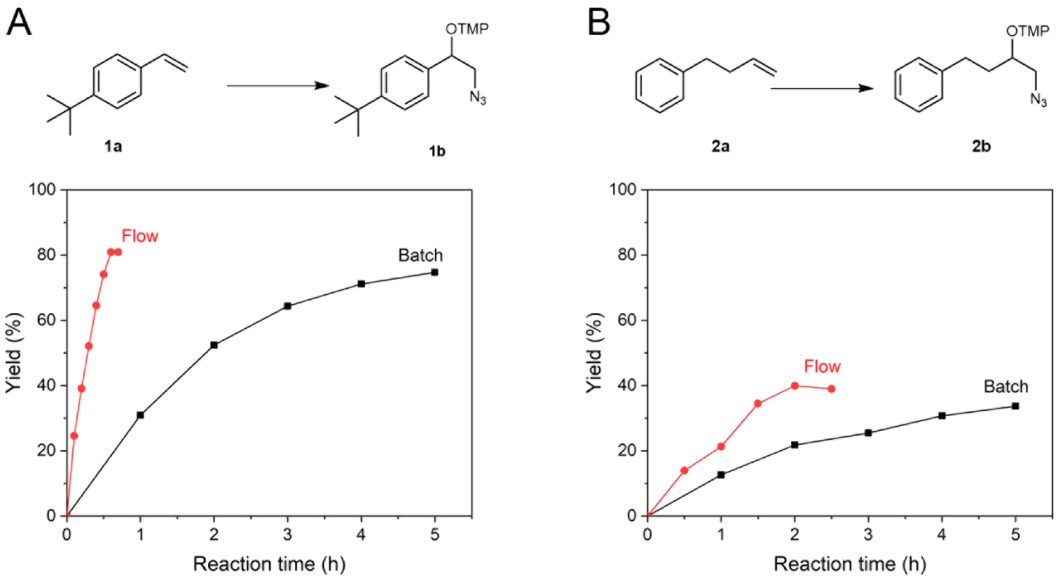

Figure 9. Comparison of the yield for the azidooxygenation reaction in the batch reactor and flow cell versus reaction time with different substrates: (A) 4-*tert*-butylstyrene (**1a**) and (B) 4-phenyl-1-butene (**2a**). The products are 1-(2-azido-1-(4-(*tert*-butyl)phenyl)ethoxy)-2,2,6,6-tetramethylpiperidine (**1b**) and 1-((1-azido-4-phenylbutan-2-yl)oxy)-2,2,6,6-tetramethylpiperidine (**2b**). The batch reactor utilized a CP anode. The flow cell utilized a MNC anode with a flow rate of 2 mL/min.

(2.67 h with washing steps) and a productivity of 0.16 mmol/h, 3.2 times higher than batch reaction (see Figure 9B, as well as Figure S12B in the Supporting Information). Therefore, we can conclude that the combination of the flow reactor with the MNC electrode can, without further optimization, dramatically improve the reaction rate for substrates that are more difficult to convert.

CONCLUSION

This work explored how the use of flow-through electrodes could improve the productivity of TEMPO-mediated azidooxygenation. Using a commercially available CP electrode, a flow reactor increased the reaction productivity by up to 3.8 times relative to a batch process because of improved transport of reactant to the electrode surface. By utilizing a flow reactor with a custom MNC electrode, the productivity of azidooxygenation could be further improved to be 7.8 times greater than that of the batch reaction with CP. This improvement was due to the higher surface area of the MNC electrode. While the batch reactor achieved a 75% yield in 5 h, the flow reactor with the MNC electrode obtained an 81% yield in 36 min, a production rate of 0.72 g h^{-1} per cm^2 of electrode area. This production rate per cm^2 of electrode area represents a 3-fold increase over the highest previously reported values for an electro-organic reaction, which was achieved with flat, nonporous electrodes.[17] The same flow-through electrode and reaction conditions could be applied to dramatically improve the productivity for substrates that are relatively easy or difficult to convert. We hope the information in the article facilitates the intensification and scale-up of electro-organic reactions.

ASSOCIATED CONTENT

Supporting Information

The Supporting Information is available free of charge at xxx. The Supporting Information is available free of charge at https://pubs.acs.org/doi/10.1021/acssuschemeng.2c01525.

Additional descriptions of the material sources, the experimental procedures, as well as additional figures and tables including an image of the disassembled flow cell; the shape of the electrode; the reaction mechanism; a background $I-V$ curve; the productivity with CP under different flow rates and applied potentials; the conductivity of electrode made with different glucose concentrations; zoom-in SEM images of CP and SCP; PEKK flow cell with reference electrode; measurement of ECSA and permeability; SEM images of electrodes after the reaction; the yield of the recycling reaction without washing; pictures of the MNC electrode after the reaction with and without washing; yield versus total time in batch and flow reactors with different substrates; weight changed after each cycle; ^{1}H NMR of products; the physical properties, productivity, and conversion efficiency of various carbon electrodes (PDF)

AUTHOR INFORMATION

Corresponding Author

Benjamin J. Wiley − *Department of Chemistry, Duke University, Durham, North Carolina 27708, United States;* orcid.org/0000-0002-1314-6223; Email: benjamin.wiley@duke.edu

Authors

Shichen Guo − *Department of Chemistry, Duke University, Durham, North Carolina 27708, United States;* orcid.org/0000-0001-8864-9055

Myung Jun Kim − *Department of Chemistry, Duke University, Durham, North Carolina 27708, United States; Department of Applied Chemistry, Kyung Hee University, Yongin 17104, Republic of Korea;* orcid.org/0000-0002-9056-4904

Juno C. Siu − *Department of Chemistry and Chemical Biology, Cornell University, Ithaca, New York 14853, United States;* orcid.org/0000-0003-4675-5399

https://doi.org/10.1021/acssuschemeng.2c01525
ACS Sustainable Chem. Eng. XXXX, XXX, XXX−XXX

Natalia von Windheim − *Department of Mechanical Engineering and Materials Science, Duke University, Durham, North Carolina 27708, United States*

Ken Gall − *Department of Mechanical Engineering and Materials Science, Duke University, Durham, North Carolina 27708, United States*

Song Lin − *Department of Chemistry and Chemical Biology, Cornell University, Ithaca, New York 14853, United States;* orcid.org/0000-0002-8880-6476

Complete contact information is available at: https://pubs.acs.org/10.1021/acssuschemeng.2c01525

Notes

The authors declare no competing financial interest.

■ ACKNOWLEDGMENTS

Acknowledgment is made to the Donors of the American Chemical Society Petroleum Research Fund and NSF (No. CHE-1751839) for support of this research. SEM and conductivity measurement were performed in part at the Duke University Shared Materials Instrumentation Facility (SMIF), a member of the North Carolina Research Triangle Nanotechnology Network (RTNN), which is supported by the National Science Foundation (Award No. ECCS-2025064) as part of the National Nanotechnology Coordinated Infrastructure (NNCI). S.L. thanks the Dreyfus Foundation for a Teacher-Scholar Award and FMC for a New Investigator Award.

■ REFERENCES

(1) Frontana-Uribe, B. A.; Little, R. D.; Ibanez, J. G.; Palma, A.; Vasquez-Medrano, R. Organic electrosynthesis: a promising green methodology in organic chemistry. *Green Chem.* **2010**, *12*, 2099−2119.

(2) Schäfer, H. J.; Harenbrock, M.; Klocke, E.; Plate, M.; Weiper-Idelmann, A. Electrolysis for the benign conversion of renewable feedstocks. *Pure Appl. Chem.* **2007**, *79*, 2047−2057.

(3) Yan, M.; Kawamata, Y.; Baran, P. S. Synthetic Organic Electrochemical Methods Since 2000: On the Verge of a Renaissance. *Chem. Rev.* **2017**, *117*, 13230−13319.

(4) Wiebe, A.; Gieshoff, T.; Möhle, S.; Rodrigo, E.; Zirbes, M.; Waldvogel, S. R. Electrifying Organic Synthesis. *Angew. Chem., Int. Ed.* **2018**, *57*, 5594−5619.

(5) Horn, E. J.; Rosen, B. R.; Baran, P. S. Synthetic Organic Electrochemistry: An Enabling and Innately Sustainable Method. *ACS Cent. Sci.* **2016**, *2*, 302−308.

(6) Siu, J. C.; Fu, N.; Lin, S. Catalyzing Electrosynthesis: A Homogeneous Electrocatalytic Approach to Reaction Discovery. *Acc. Chem. Res.* **2020**, *53*, 547−560.

(7) Novaes, L. F. T.; Liu, J.; Shen, Y.; Lu, L.; Meinhardt, J. M.; Lin, S. Electrocatalysis as an enabling technology for organic synthesis. *Chem. Soc. Rev.* **2021**, *50*, 7941−8002.

(8) Fu, N.; Sauer, G. S.; Saha, A.; Loo, A.; Lin, S. Metal-catalyzed electrochemical diazidation of alkenes. *Science* **2017**, *357*, 575.

(9) Peters, B. K.; Rodriguez, K. X.; Reisberg, S. H.; Beil, S. B.; Hickey, D. P.; Kawamata, Y.; Collins, M.; Starr, J.; Chen, L.; Udyavara, S.; Klunder, K.; Gorey, T. J.; Anderson, S. L.; Neurock, M.; Minteer, S. D.; Baran, P. S. Scalable and safe synthetic organic electroreduction inspired by Li-ion battery chemistry. *Science* **2019**, *363*, 838.

(10) Siu, T.; Li, W.; Yudin, A. K. Parallel Electrosynthesis of α-Alkoxycarbamates, α-Alkoxyamides, and α-Alkoxysulfonamides Using the Spatially Addressable Electrolysis Platform (SAEP). *J. Comb. Chem.* **2000**, *2*, 545−549.

(11) Gütz, C.; Klöckner, B.; Waldvogel, S. R. Electrochemical Screening for Electroorganic Synthesis. *Org. Process Res. Dev.* **2016**, *20*, 26−32.

(12) Li, C.; Kawamata, Y.; Nakamura, H.; Vantourout, J. C.; Liu, Z.; Hou, Q.; Bao, D.; Starr, J. T.; Chen, J.; Yan, M.; Baran, P. S. Electrochemically Enabled, Nickel-Catalyzed Amination. *Angew. Chem., Int. Ed.* **2017**, *56*, 13088−13093.

(13) Yan, M.; Kawamata, Y.; Baran, P. S. Synthetic Organic Electrochemistry: Calling All Engineers. *Angew. Chem., Int. Ed.* **2018**, *57*, 4149−4155.

(14) Rein, J.; Annand, J. R.; Wismer, M. K.; Fu, J.; Siu, J. C.; Klapars, A.; Strotman, N. A.; Kalyani, D.; Lehnherr, D.; Lin, S. Unlocking the Potential of High-Throughput Experimentation for Electrochemistry with a Standardized Microscale Reactor. *ACS Cent. Sci.* **2021**, *7*, 1347−1355.

(15) Halford, B. Amping up the pharma lab: Drug companies explore the potential of electrochemistry 2019. Available via the Internet at: https://cen.acs.org/synthesis/medicinal-chemistry/Amping-pharma-lab-Drug-companies/97/i43.

(16) Pletcher, D.; Green, R. A.; Brown, R. C. D. Flow Electrolysis Cells for the Synthetic Organic Chemistry Laboratory. *Chem. Rev.* **2018**, *118*, 4573−4591.

(17) Green, R. A.; Brown, R. C. D.; Pletcher, D. Electrosynthesis in extended channel length microfluidic electrolysis cells. *J. Flow Chem.* **2016**, *6*, 191−197.

(18) Gütz, C.; Stenglein, A.; Waldvogel, S. R. Highly Modular Flow Cell for Electroorganic Synthesis. *Org. Process Res. Dev.* **2017**, *21*, 771−778.

(19) Noel, T.; Cao, Y.; Laudadio, G. The Fundamentals Behind the Use of Flow Reactors in Electrochemistry. *Acc. Chem. Res.* **2019**, *52*, 2858−2869.

(20) Jud, W.; Kappe, C. O.; Cantillo, D. Development and Assembly of a Flow Cell for Single-Pass Continuous Electroorganic Synthesis Using Laser-Cut Components. *Chem.−Methods* **2021**, *1*, 36−41.

(21) Perry, S. C.; Ponce de León, C.; Walsh, F. C. Review—The Design, Performance and Continuing Development of Electrochemical Reactors for Clean Electrosynthesis. *J. Electrochem. Soc.* **2020**, *167*, 155525.

(22) Burnett, R. W. Electrochemical characteristics of the gold micromesh electrode. *Anal. Chem.* **1973**, *45*, 258−263.

(23) Langlois, S.; Coeuret, F. Flow-through and flow-by porous electrodes of nickel foam. I. Material characterization. *J. Appl. Electrochem.* **1989**, *19*, 43−50.

(24) Delanghe, B.; Tellier, S.; Astruc, M. Mass transfer to a carbon or graphite felt electrode. *Electrochim. Acta* **1990**, *35*, 1369−1376.

(25) Kinoshita, K.; Leach, S. C. Mass-Transfer Study of Carbon Felt, Flow-Through Electrode. *J. Electrochem. Soc.* **1982**, *129*, 1993−1997.

(26) Kordesch, K.; Jahangir, S.; Schautz, M. Engineering concepts and technical performance of oxygen-reducing electrodes for batteries and electrochemical processes. *Electrochim. Acta* **1984**, *29*, 1589−1596.

(27) Blaedel, W.; Wang, J. Flow electrolysis on a reticulated vitreous carbon electrode. *Anal. Chem.* **1979**, *51*, 799−802.

(28) Strohl, A.; Curran, D. Reticulated vitreous carbon flow-through electrodes. *Anal. Chem.* **1979**, *51*, 353−357.

(29) Wang, J. Reticulated vitreous carbon—a new versatile electrode material. *Electrochim. Acta* **1981**, *26*, 1721−1726.

(30) Bard, A. J.; Faulkner, L. R. *Electrochemical Methods: Fundamentals and Applications*, 2nd Edition; John Wiley & Sons, 2000; pp 87−132.

(31) Kim, M. J.; Seo, Y.; Cruz, M. A.; Wiley, B. J. Metal Nanowire Felt as a Flow-Through Electrode for High-Productivity Electrochemistry. *ACS Nano* **2019**, *13*, 6998−7009.

(32) Walsh, F. C.; Pletcher, D. *Electrochemical Engineering and Cell Design*; John Wiley & Sons, Ltd., 2014; pp 95−111.

(33) Ralph, T. R.; Hitchman, M. L.; Millington, J. P.; Walsh, F. C. The Importance of Batch Electrolysis Conditions during the Reduction of L-Cystine Hydrochloride. *J. Electrochem. Soc.* **2005**, *152*, D54.

(34) Walsh, F. C.; Ponce de León, C. Progress in electrochemical flow reactors for laboratory and pilot scale processing. *Electrochim. Acta* **2018**, *280*, 121−148.
(35) Arenas, L. F.; Ponce de León, C.; Walsh, F. C. Three-dimensional porous metal electrodes: Fabrication, characterisation and use. *Curr. Opin. Electrochem.* **2019**, *16*, 1−9.
(36) Nutting, J. E.; Rafiee, M.; Stahl, S. S. Tetramethylpiperidine N-Oxyl (TEMPO), Phthalimide N-Oxyl (PINO), and Related N-Oxyl Species: Electrochemical Properties and Their Use in Electrocatalytic Reactions. *Chem. Rev.* **2018**, *118*, 4834−4885.
(37) Siu, J. C.; Sauer, G. S.; Saha, A.; Macey, R. L.; Fu, N.; Chauvire, T.; Lancaster, K. M.; Lin, S. Electrochemical Azidooxygenation of Alkenes Mediated by a TEMPO-N_3 Charge-Transfer Complex. *J. Am. Chem. Soc.* **2018**, *140*, 12511−12520.
(38) Zhao, H.-B.; Xu, P.; Song, J.; Xu, H.-C. Cathode Material Determines Product Selectivity for Electrochemical C−H Functionalization of Biaryl Ketoximes. *Angew. Chem., Int. Ed.* **2018**, *57*, 15153−15156.
(39) Bergmeier, S. C. The synthesis of vicinal amino alcohols. *Tetrahedron* **2000**, *56*, 2561−2576.
(40) Zhang, B.; Studer, A. Stereoselective Radical Azidooxygenation of Alkenes. *Org. Lett.* **2013**, *15*, 4548−4551.
(41) Reddy, T. R.; Rao, D. S.; Kashyap, S. Visible-light activated metal catalyst-free vicinal diazidation of olefins with sulfonium iodate(I) species. *Chem. Commun.* **2019**, *55*, 2833−2836.
(42) Kösel, T.; Schulz, G.; Dräger, G.; Kirschning, A. Photochemical Transformations with Iodine Azide after Release from an Ion-Exchange Resin. *Angew. Chem., Int. Ed.* **2020**, *59*, 12376−12380.
(43) Kawamata, Y.; Yan, M.; Liu, Z.; Bao, D. H.; Chen, J.; Starr, J. T.; Baran, P. S. Scalable, Electrochemical Oxidation of Unactivated C-H Bonds. *J. Am. Chem. Soc.* **2017**, *139*, 7448−7451.
(44) Laudadio, G.; Barmpoutsis, E.; Schotten, C.; Struik, L.; Govaerts, S.; Browne, D. L.; Noel, T. Sulfonamide Synthesis through Electrochemical Oxidative Coupling of Amines and Thiols. *J. Am. Chem. Soc.* **2019**, *141*, 5664−5668.
(45) Laudadio, G.; Bartolomeu, A. A.; Verwijlen, L.; Cao, Y.; de Oliveira, K. T.; Noel, T. Sulfonyl Fluoride Synthesis through Electrochemical Oxidative Coupling of Thiols and Potassium Fluoride. *J. Am. Chem. Soc.* **2019**, *141*, 11832−11836.
(46) Zhang, W.; Lin, S. Electroreductive Carbofunctionalization of Alkenes with Alkyl Bromides via a Radical-Polar Crossover Mechanism. *J. Am. Chem. Soc.* **2020**, *142*, 20661−20670.
(47) Pasciak, E. M.; Rittichier, J. T.; Chen, C.-H.; Mubarak, M. S.; VanNieuwenhze, M. S.; Peters, D. G. Electroreductive Dimerization of Coumarin and Coumarin Analogues at Carbon Cathodes. *J. Org. Chem.* **2015**, *80*, 274−280.
(48) Amemiya, F.; Kashiwagi, T.; Fuchigami, T.; Atobe, M. Electrochemical Conversion of Benzylamine to Dibenzylamine Using a Microreactor: Analogous System of Photocatalytic Redox Combined Synthesis. *Chem. Lett.* **2011**, *40*, 606−608.
(49) Heard, D. M.; Lennox, A. J. J. Electrode Materials in Modern Organic Electrochemistry. *Angew. Chem., Int. Ed.* **2020**, *59*, 18866−18884.
(50) Leung, P.; Shah, A. A.; Sanz, L.; Flox, C.; Morante, J. R.; Xu, Q.; Mohamed, M. R.; Ponce de León, C.; Walsh, F. C. Recent developments in organic redox flow batteries: A critical review. *J. Power Sources* **2017**, *360*, 243−283.
(51) Huskinson, B.; Marshak, M. P.; Suh, C.; Er, S.; Gerhardt, M. R.; Galvin, C. J.; Chen, X.; Aspuru-Guzik, A.; Gordon, R. G.; Aziz, M. J. A metal-free organic−inorganic aqueous flow battery. *Nature* **2014**, *505*, 195−198.
(52) Lin, K.; Gómez-Bombarelli, R.; Beh, E. S.; Tong, L.; Chen, Q.; Valle, A.; Aspuru-Guzik, A.; Aziz, M. J.; Gordon, R. G. A redox-flow battery with an alloxazine-based organic electrolyte. *Nat. Energy* **2016**, *1*, 16102.
(53) Winsberg, J.; Janoschka, T.; Morgenstern, S.; Hagemann, T.; Muench, S.; Hauffman, G.; Gohy, J.-F.; Hager, M. D.; Schubert, U. S. Poly(TEMPO)/Zinc Hybrid-Flow Battery: A Novel, "Green," High Voltage, and Safe Energy Storage System. *Adv. Mater.* **2016**, *28*, 2238−2243.
(54) Lin, K.; Chen, Q.; Gerhardt, M. R.; Tong, L.; Kim, S. B.; Eisenach, L.; Valle, A. W.; Hardee, D.; Gordon, R. G.; Aziz, M. J.; Marshak, M. P. Alkaline quinone flow battery. *Science* **2015**, *349*, 1529−1532.
(55) Nelson, H. M.; Siu, J. C.; Saha, A.; Cascio, D.; MacMillan, S. N.; Wu, S.-B.; Lu, C.; Rodríguez, J. A.; Houk, K. N.; Lin, S. Isolation and X-ray Crystal Structure of an Electrogenerated TEMPO−N_3 Charge-Transfer Complex. *Org. Lett.* **2021**, *23*, 454−458.
(56) Schmal, D.; Van Erkel, J.; Van Duin, P. Mass transfer at carbon fibre electrodes. *J. Appl. Electrochem.* **1986**, *16*, 422−430.
(57) Lizarraga, D.; Bisang, J. Mass transfer studies at iron felts. *J. Appl. Electrochem.* **1996**, *26*, 1209−1215.
(58) Rezk, K.; Forsberg, J.; Nilsson, L.; Berghel, J. Characterizing flow resistance in 3-dimensional disordered fibrous structures based on Forchheimer coefficients for a wide range of Reynolds numbers. *Appl. Math. Model.* **2016**, *40*, 8898−8911.
(59) Fuertes, A. B.; Alvarez, S. Graphitic mesoporous carbons synthesised through mesostructured silica templates. *Carbon* **2004**, *42*, 3049−3055.
(60) Hishiyama, Y.; Inagaki, M.; Kimura, S. Graphitization of carbon fibre/glassy carbon composites. *Carbon* **1974**, *12*, 249−258.
(61) Barbera, K.; Frusteri, L.; Italiano, G.; Spadaro, L.; Frusteri, F.; Perathoner, S.; Centi, G. Low-temperature graphitization of amorphous carbon nanospheres. *Chin. J. Catal.* **2014**, *35*, 869−876.
(62) Toray Carbon Paper 120, Wet Proofed. Available via the Internet at: https://www.fuelcellstore.com/toray-carbon-paper-120 (accessed Mar. 2022).
(63) Forner-Cuenca, A.; Penn, E. E.; Oliveira, A. M.; Brushett, F. R. Exploring the Role of Electrode Microstructure on the Performance of Non-Aqueous Redox Flow Batteries. *J. Electrochem. Soc.* **2019**, *166*, A2230−A2241.
(64) Li, S.; Ceccato, M.; Lu, X.; Frank, S.; Lock, N.; Roldan, A.; Hu, X.-M.; Skrydstrup, T.; Daasbjerg, K. Incorporation of nickel single atoms into carbon paper as self-standing electrocatalyst for CO_2 reduction. *J. Mater. Chem. A* **2021**, *9*, 1583−1592.
(65) Choi, M. A.; Lee, M. H.; Chang, J.; Lee, S. J. Permeability modeling of fibrous media in composite processing. *J. Nonnewton. Fluid Mech.* **1998**, *79*, 585−598.
(66) Tomadakis, M. M.; Robertson, T. J. Viscous Permeability of Random Fiber Structures: Comparison of Electrical and Diffusional Estimates with Experimental and Analytical Results. *J. Compos. Mater.* **2005**, *39*, 163−188.
(67) Cai, J.; Luo, L.; Ye, R.; Zeng, X.; Hu, X. Recent Advances on Fractal Modeling of Permeability for Fibrous Porous Media. *Fractals* **2015**, *23*, 1540006.

https://doi.org/10.1021/acssuschemeng.2c01525
ACS Sustainable Chem. Eng. XXXX, XXX, XXX−XXX